frontiers in Materials

ORIGINAL RESEARCH
published: 12 August 2021
doi: 10.3389/fmats.2021.719536

Biomechanical Properties of 3D-Printed Cervical Interbody Fusion Cage With Novel SF/nHAp Composites

*Shuang Chen[1†], Yi Meng[1†], Guozhi Wu[1†], Zhize Liu[1], Xiaodong Lian[1], Jianyu Hu[1], Dongfang Yang[1], Guiqi Zhang[1], Kun Li[2] and Hao Zhang[1]**

[1]Department of Orthopedics, Affiliated Dalian Municipal Central Hospital, Dalian Medical University, Dalian, China, [2]Department of Orthopedics, The Peoples Hospital of Langfang City, Langfang, China

Anterior cervical discectomy and fusion (ACDF) is a commonly used surgical method for the treatment of cervical spondylosis. As ACDF surgery is widely used in clinics, identifying suitable materials to design and prepare cervical interbody fusion cages is a hot research topic. Here, we describe a new three-dimensional (3D) printing approach to create stretchable and tough silk fibroin/nano-hydroxyapatite (SF/nHAp) composites with tunable mechanical properties. The compressive strength of the novel composites with biomimetic structure could reach more than 128 MPa. More importantly, the composites were prepared using 30% silk fibroin and 70% hydroxyapatite, a composition similar to the human bone tissue. Finite element analysis results indicate that the stress distribution of SF/nHAp composite cervical interbody fusion cages *in vivo* is more uniform than that of commercial Ti alloy cages. This study evaluates the effectiveness of SF/nHAp composites for application in cervical interbody fusion cages and in the field of bone tissue engineering.

Keywords: 3D printing, cervical interbody fusion cages, biomechanical properties, silk fibroin, nano-hydroxyapatite, composites

OPEN ACCESS

Edited by:
Xufeng Dong,
Dalian University of Technology, China

Reviewed by:
Ying Hu,
Hefei University of Technology, China
Qingyu Peng,
Harbin Institute of Technology, China

****Correspondence:***
Hao Zhang
691248842@qq.com

[†]These authors have contributed equally to this work

Specialty section:
This article was submitted to Polymeric and Composite Materials, a section of the journal Frontiers in Materials

Received: *02 June 2021*
Accepted: *29 June 2021*
Published: *12 August 2021*

Citation:
Chen S, Meng Y, Wu G, Liu Z, Lian X, Hu J, Yang D, Zhang G, Li K and Zhang H (2021) Biomechanical Properties of 3D-Printed Cervical Interbody Fusion Cage With Novel SF/nHAp Composites. Front. Mater. 8:719536. doi: 10.3389/fmats.2021.719536

INTRODUCTION

In cervical fusion surgery, it is always difficult to choose the appropriate bone implant (Park and Roh, 2013; Ming et al., 2015; Mazas et al., 2019). A bone tissue engineering scaffold not only plays the role of structural support in a human body but is also beneficial for cell adhesion, growth, and reproduction, providing a place for tissue regeneration and plasticity (Dias et al., 2021; Su et al., 2021). Therefore, bone tissue engineering scaffold materials should have good biocompatibility, degradability, osteoinduction, certain compressive strength, and toughness to meet the requirements of cell proliferation and differentiation on the surface of materials (Ming et al., 2015; Wei et al., 2019).

Currently, inorganic composite materials occupy a very important place in the research of bone tissue engineering scaffold materials. Among these inorganic materials, hydroxyapatite, the main component of human bones and teeth, has good biocompatibility and is a commonly used hard tissue material that can perfectly combine with human bones and induce the formation of new bones (Cho et al., 2017; Pitjamit et al., 2020; Thunsiri et al., 2020). However, a single hydroxyapatite particle has inherent defects such as high brittleness and low bending strength, which limit its further application in bone tissue engineering. Currently, the most commonly used method to improve the comprehensive properties of hydroxyapatite is by compounding it with metals and ceramics (Jin et al., 2014; Farokhi et al., 2018). However, hydroxyapatite/metal composites have some problems, such as metal corrosion, dense fibrous tissue, and stress shielding at the bone–graft interface (Larobina et al., 2012; Ming et al., 2015; Campo et al., 2017; Deng et al., 2017). However, hydroxyapatite/polymer composites have gradually become a

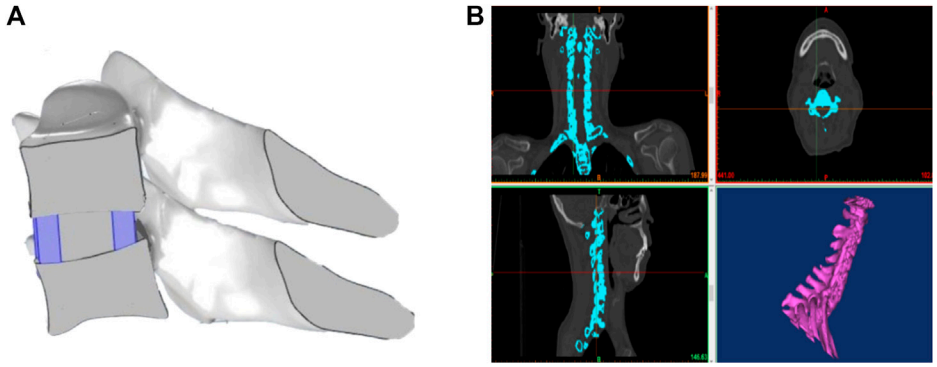

FIGURE 1 | (A) 3D model of the cervical interbody fusion cage obtained by Mimics. **(B)** Original 3D CT image of the cervical spine scanned from a healthy woman.

research hotspot because of their advantages of no tissue reaction, no inhibition of bone growth, and no need of secondary surgery (Jin et al., 2014; Cho et al., 2017; Farokhi et al., 2018).

With the rapid development of nanotechnology, the application of nano-hydroxyapatite is becoming more extensive. The nanostructure of nano-hydroxyapatite can provide an amazing interface effect, significantly improving its biomechanical strength and increasing its surface bioactivity (Ruan et al., 2018). In addition, some polymers, including synthetic and natural polymers, with good flexibility and degradability have gradually gained attention as promising candidate materials for compounding with hydroxyapatite (Hassanajili et al., 2019; Pei et al., 2019; Cakmak et al., 2020). Compared with synthetic polymers, natural polymers have attracted more attention in bone tissue engineering due to their unique biocompatibility and biodegradability. Chen et al. made a kind of bone implant material with nano-hydroxyapatite/collagen composite material which has high biocompatibility and strong biomechanical properties, and is an ideal bone tissue engineering scaffold choice (Chen et al., 2016). However, collagen materials are mainly extracted from animals or synthesized artificially, which makes it difficult to be widely used in experimental research and clinical practice (Sun et al., 2016; Kambe et al., 2017). Among natural polymers, silk fibroin derived from silk is a natural high-purity protein composed of a variety of amino acids and has a clear sequence of amino acids, and this natural polymer has high safety, which can eliminate the potential immune sensitization (Jin et al., 2014; Gholipourmalekabadi et al., 2015). The most striking feature is that silk fibroin also has excellent biological activity, which can support the adsorption, adhesion, diffusion, and differentiation of various cells on its surface (Ruan et al., 2018). In addition, silk fibroin has excellent vascular induction ability, which further promotes the repair of surrounding tissues. These excellent properties make silk fibroin an ideal choice to replace collagen (Kambe et al., 2017).

In this work, we constructed a composite material for bone tissue engineering by combining silk fibroin (SF) with nano-hydroxyapatite (nHAp) and prepared a cervical interbody fusion cage by 3D printing. The mechanical properties of the SF/nHAp composite cage were tested, and finite element analysis was conducted to compare the biomechanical properties of the SF/nHAp cage and commercial Ti alloy cages.

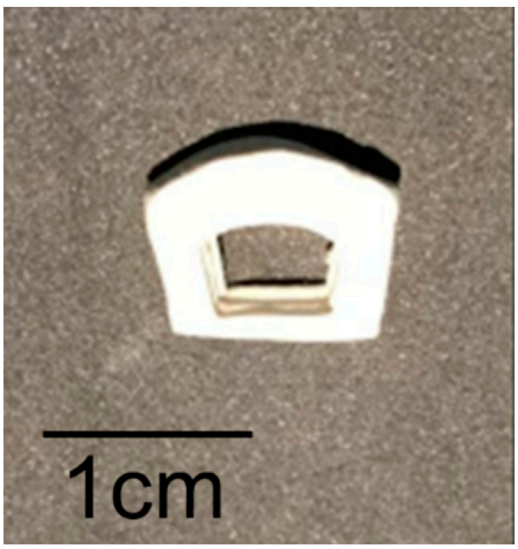

FIGURE 2 | Photos of the 3D-printed cervical interbody fusion cage.

MATERIALS AND METHODS

Materials

Silk fibroin was purchased from the Institute of Chemistry, Chinese Academy of Sciences; nano-hydroxyapatite was obtained from Beijing Deco Island Gold Technology Co., Ltd. Sodium carbonate, calcium chloride, ethanol, deionized water, diammonium hydrogen phosphate, and ammonia water were all purchased from Sinopharm Chemical Reagent Co., Ltd. (China) and used as received without further purification.

Fabrication of Silk Fibroin

First, 0.5% sodium carbonate solution in a beaker was heated to a slight boiling point, 15 g silk was added and the mixture stirred

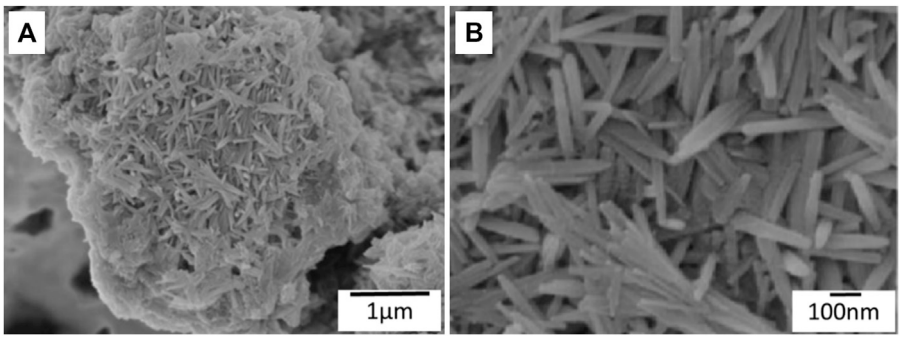

FIGURE 3 | (A) SEM images showing nano-hydroxyapatite needles formed on the silk fibroin substrate. **(B)** High magnification of SEM images of nano-hydroxyapatite needles.

for 0.5 h, the mixture was rinsed with deionized water, the above process was repeated for secondary degumming, and then the mixture was allowed to dry naturally. The degummed silk fibroin was weighed. Then, 13.8 g degummed silk fibroin was added into a ternary system of calcium chloride, ethanol, and water at a molar ratio of 1:2:8 and dissolved at 60°C for 2 h. After dissolution, 1.5 times deionized water (heated to 60°C in advance) was added, the mixture cooled to room temperature, filtered with a filter membrane, and transferred into a dialysis bag for dialysis for 3–5 days to obtain silk fibroin (SF) material (Huang et al., 2019).

Preparation of SF/nHAp Composites

15 g silk was soaked in 0.5% sodium carbonate solution (90°C) for 0.5 h, and then the aforementioned process was repeated for secondary degumming. Then, the mixture was air-dried naturally to obtain degummed silk fibroin. 3.25 g of degummed silk fibroin was dissolved in 36.5 ml of calcium chloride, ethanol, and water at a molar ratio of 1:2:8 at 60°C; temperature was adjusted to 75°C; and diammonium hydrogen phosphate solution was added dropwise. After 24 h, the product was washed with deionized water and freeze-dried to obtain SF/nHAp composites.

Cervical Interbody Fusion Cage Fabricated With 3D Printing Technique

A 3D bioprinter (EFD company, 2400) was used to prepare the 3D printing cage. The 3D model (**Figure 1A**) of the cage that was supposed to be implanted between C5 and C6 was obtained by Mimics. The original 3D CT image of the cervical spine (**Figure 1B**) was scanned from a healthy woman, who is 55 years old, 165 cm tall, and 70 kg in weight.

The prepared SF/nHAp composites were loaded into a syringe and centrifuged to exhaust air. Under the condition of pressure of 15Psi and linearity of 8 mm/s, 3D direct writing printing and layer-by-layer printing were carried out to make the cervical interbody fusion cage. The 3D printing cervical interbody fusion cage was soaked in 5% calcium chloride–water–ethanol solution for one night and dried naturally to obtain the cervical interbody fusion cage, as shown in **Figure 2**.

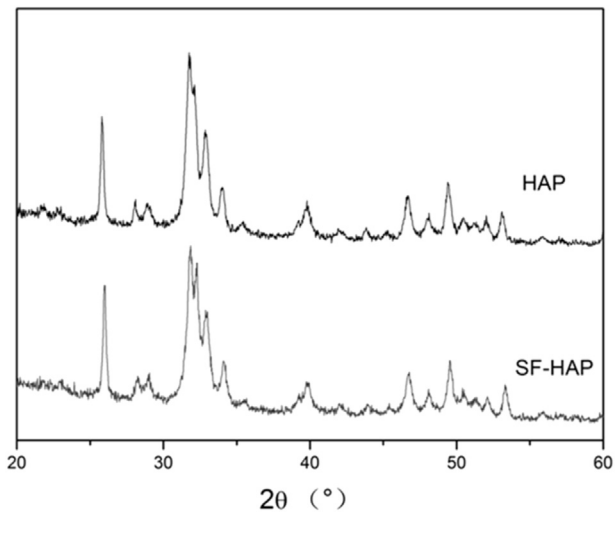

FIGURE 4 | XRD patterns of the pure HAp and SF/nHAp composites.

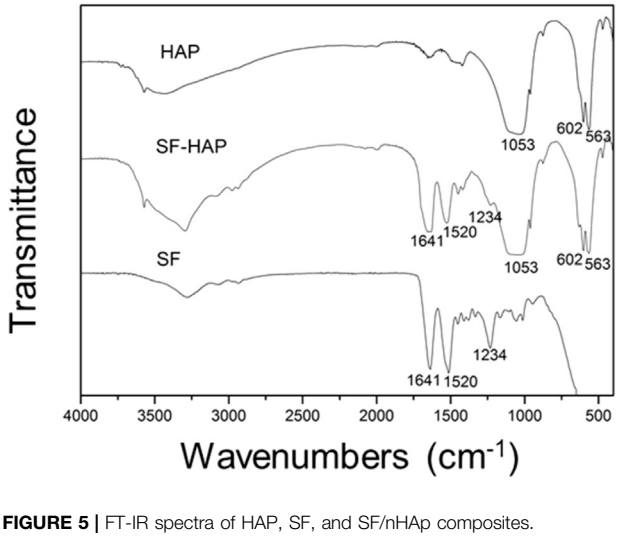

FIGURE 5 | FT-IR spectra of HAP, SF, and SF/nHAp composites.

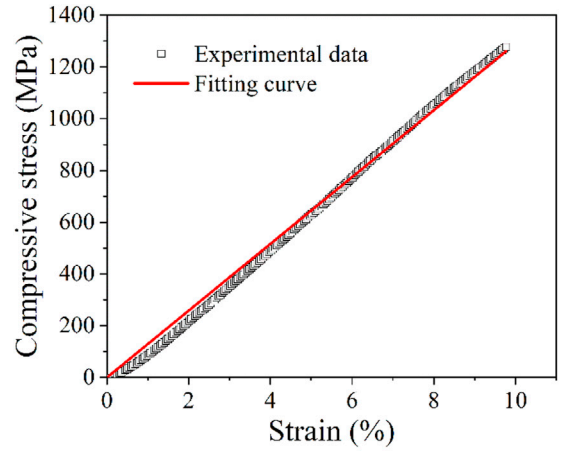

FIGURE 6 | Compression curve of SF/nHAp composites.

TABLE 1 | Mechanical properties of model components.

Model components	Young's modulus (GPa)	Poisson's ratio
Cortical bone	12	0.29
Cancellous bone	0.1	0.29
SF/nHAp composite cage	12.9	0.29
Titanium alloy cage	110	0.29

Characterization of SF/nHAp Composites

The crystalline structures and chemical compositions of the SF/nHAp composites were examined by X-ray diffraction (XRD; Empyrean, Panaco) and Fourier transform infrared spectroscopy (FTIR; iS10, Thermo Fisher Scientific). The morphologies of the SF/nHAp composites were determined by scanning electron microscopy (SEM; JSM7500F, JEOL).

Mechanical Property Testing of SF/nHAp Composites

An electronic universal material testing machine (Instron 3365, Instron) was used to test the compressive properties of the SF/nHAp composites. The unconstrained sample, with size 12.7 × 12.7 × 25.4 mm, was compressed between flat steel plates at a constant strain rate of 1 mm/min.

RESULTS AND DISCUSSION

The SEM images (**Figure 3** show the formation of nano-hydroxyapatite needles on the silk fibroin substrate. The length and width of the nano-hydroxyapatite needles are ~400 and ~24 nm, respectively.

Figure 4 presents the XRD patterns of the pure HAp and SF/nHAp composites. The XRD pattern shows that the peak position of SF/nHAp is the same as that of pure HAP, and there is no other phosphate diffraction peak, indicating that hydroxyapatite crystals are formed. It could be proved that although the silk fibroin material is present in the SF/nHAp composite material, it does not affect the formation of hydroxyapatite crystals in the composite material. In addition, the bottom of the SF/nHAp diffraction peak is broad and not sharp.

The FT-IR results show that SF/nHAp composites are formed, as shown in **Figure 5**. Among them, 1,053, 602,, and 563 cm^{-1} correspond to the characteristic peak of phosphate, indicating that the compositional and structural properties of hydroxyapatite are present in the composites, and 1,641, 1,520, and 1,234 cm^{-1} correspond to the characteristic peaks of amide I, II, and III, respectively, in the silk fibroin structure. Based on the above analysis, it can be seen that the structure and properties of SF/nHAp composites are clear.

With the development of nanotechnology, nano-hydroxyapatite with ultra-fine and nanostructures is being widely studied. Nano-hydroxyapatite materials can reduce the sintering temperature, improve the surface and interface effects of the nanomaterials, and degrade and absorb in the biological environment in the human body. Because of the excellent properties of silk fibroin and nano-hydroxyapatite materials, more and more research studies have used silk fibroin as a scaffold material combined with hydroxyapatite to make spinal intervertebral fusion cages. In this study, we successfully prepared SF/nHAp composites containing 30% silk

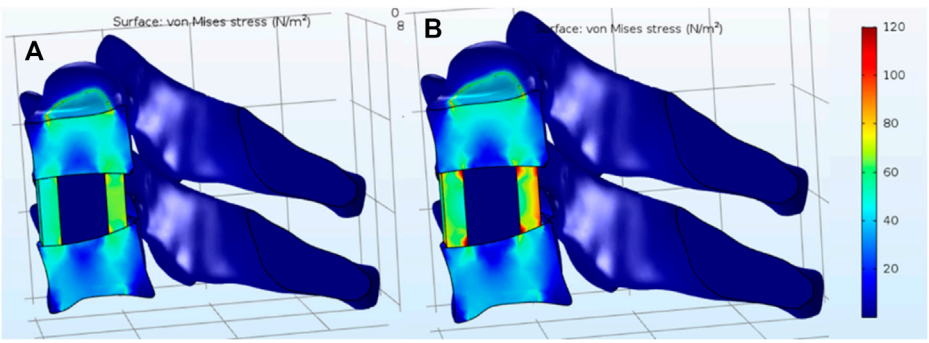

FIGURE 7 | Stress distribution under standing condition. **(A)** SF/nHAp composite cage. **(B)** Ti alloy cage.

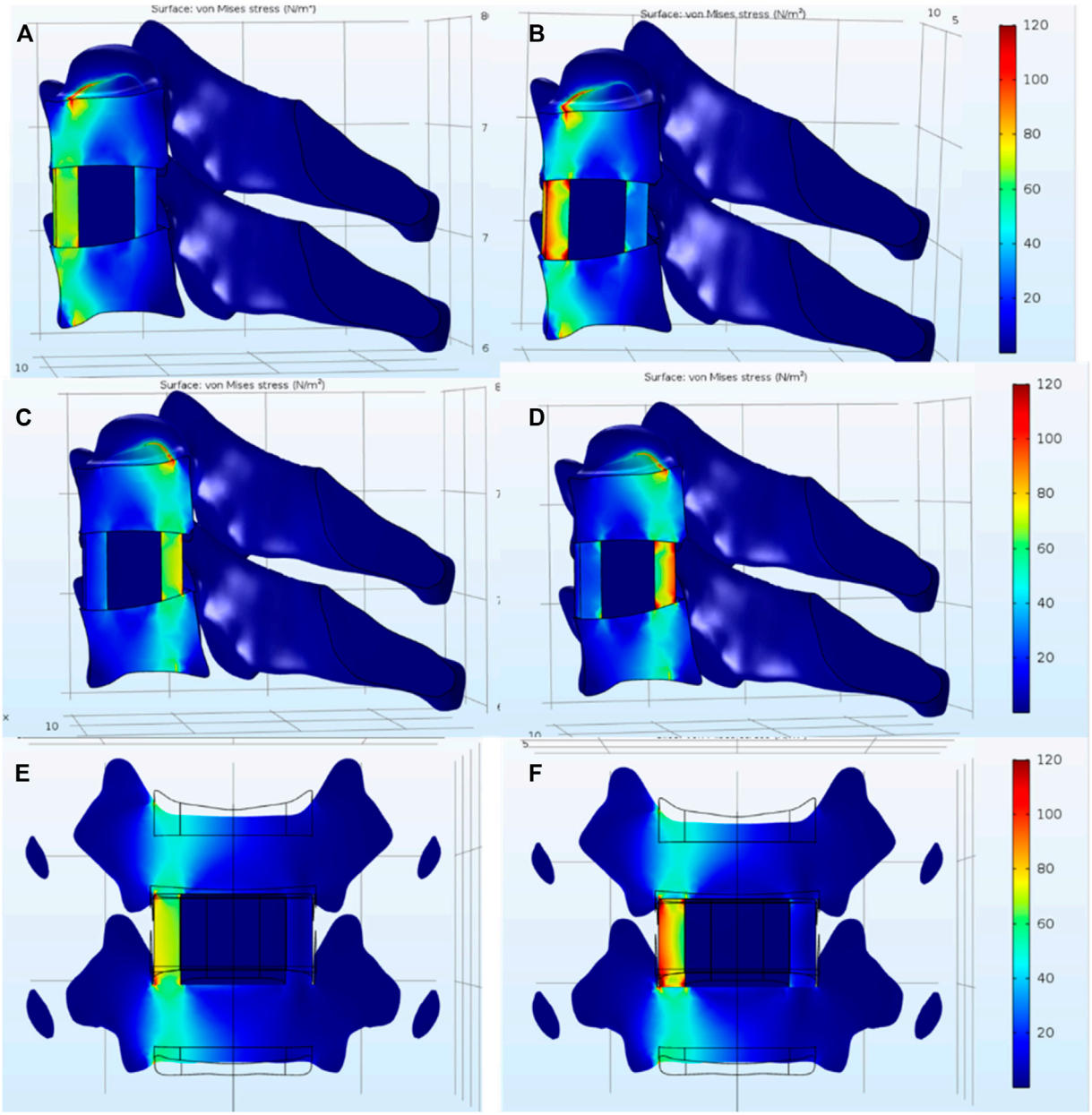

FIGURE 8 | Stress distribution under **(A)** anteflexion, **(C)** retro-extension, and **(E)** side bend with a SF/nHAp composite cage. Stress distribution under **(B)** anteflexion, **(D)** retro-extension, and **(F)** side bend with a Ti alloy cage.

fibroin and 70% hydroxyapatite. The composition (Ca/P ratio 1.67) is similar to that in the human bone tissue (Ca/P ratio 1.67).

The compression curve of the SF/nHAp composites is shown in **Figure 6**. The compressive stress linearly increases with increasing strain. The compressive stress at 9.77% strain is 1.28 GPa. The composite did not yield at ~10%, which indicates that its compressive strength is higher than 1.28 GPa. The stress vs. strain curve is fitted by a linear equation. Young's modulus of the composites is 12.9 GPa, which can be obtained as the slope of the fitting curve.

FINITE ELEMENT ANALYSIS

To compare the mechanical behavior of the SF/nHAp composite cage and commercial titanium alloy cages, a finite element model was established by using COMSOL Multiphysics. The mechanical properties of the model components are listed in **Table 1**.

Generally, the mass of a human head is 7% of the person's total body mass. Therefore, the weight of a woman's head is ~52N. It can be deduced that the moment applied on the C5 cervical vertebra is 1.8N•m. The stress distribution after implanting the cage is analyzed under various conditions, including standing,

anteflexion, retro-extension, and side bend. As shown in **Figure 7**, under standing condition, the stress distributes uniformly in the SF/nHAp composite cage, while the stress concentration can be observed on the edge of the end plate when the Ti alloy cage is implanted.

Figure 8 shows the stress distribution under anteflexion, retro-extension, and side bend. By comparison, the stress concentration in the SF/nHAp composite cage is less significant than that in the Ti alloy cage. The results indicate that by using SF/nHAp composites with similar mechanical properties as the natural bone, stress concentration could be reduced compared to that using traditional Ti alloys.

CONCLUSION

In this study, a novel 3D-printed SF/nHAp composite scaffold was fabricated by using the direct writing–based 3D printing technology. This scaffold with biomimetic structure and appropriate mechanical properties showed good biocompatibility and provided suitable templates for cervical interbody fusion cages. Importantly, composites containing 30% silk fibroin and 70% hydroxyapatite were prepared by a safe and effective mineral co-deposition method. This biomimetic preparation method could be used to successfully prepare a composition and structure similar to the human bone tissue, so it is expected that this new composite material could become the ideal object of bone implant materials that are suitable for spinal bone graft fusion in follow-up research studies. This will provide access to functional multi-materials that have applications in cervical interbody fusion cages.

DATA AVAILABILITY STATEMENT

The raw data supporting the conclusion of this article will be made available by the authors, without undue reservation.

ETHICS STATEMENT

Written informed consent was obtained from the individual(s) for the publication of any potentially identifiable images or data included in this article.

AUTHOR CONTRIBUTIONS

Conceptualization: SC and HZ; methodology: YM and GW; validation: ZL and XL; formal analysis: JH; investigation: SC; resources: DY; data curation: GZ and KL; writing—original draft preparation: SC and YM; writing—review and editing: GW and HZ; supervision: HZ; project administration: HZ; funding acquisition: HZ. All authors have read and agreed to the published version of the manuscript.

FUNDING

This research was funded by Dalian Medical Science Research Project (grant number 2011001).

REFERENCES

Cakmak, A. M., Unal, S., Sahin, A., Oktar, F. N., Sengor, M., Ekren, N., et al. (2020). 3D Printed Polycaprolactone/gelatin/bacterial Cellulose/hydroxyapatite Composite Scaffold for Bone Tissue Engineering. *Polymers* 12, 1962. doi:10.3390/polym12091962

Campo, R. D., Savoini, B., Muñoz, A., Monge, M. A., and Pareja, R. (2017). Processing and Mechanical Characteristics of Magnesium-Hydroxyapatite Metal Matrix Biocomposites. *J. Mech. Behav. Biomed. Mater.* 69, 135–143. doi:10.1016/j.jmbbm.2016.12.023

Chen, Y., Lü, G., Wang, B., Li, L., and Kuang, L. (2016). A Comparison of Anterior Cervical Discectomy and Fusion (ACDF) Using Self-Locking Stand-Alone Polyetheretherketone (PEEK) Cage with ACDF Using Cage and Plate in the Treatment of Three-Level Cervical Degenerative Spondylopathy: A Retrospective Study with 2-year Follow-Up. *Eur. Spine J.* 25, 2255–2262. doi:10.1007/s00586-016-4391-x

Cho, Y. S., Hong, M. W., Jeong, H.-J., Lee, S.-J., Kim, Y. Y., and Cho, Y.-S. (2017). The Fabrication of Well-Interconnected Polycaprolactone/hydroxyapatite Composite Scaffolds, Enhancing the Exposure of Hydroxyapatite Using the Wire-Network Molding Technique. *J. Biomed. Mater. Res.* 105, 2315–2325. doi:10.1002/jbm.b.33769

Deng, Y., Zhang, M., Chen, X., Pu, X., Liao, X., Huang, Z., et al. (2017). A Novel Akermanite/poly (Lactic-Co-Glycolic Acid) Porous Composite Scaffold Fabricated via a Solvent Casting-Particulate Leaching Method Improved by Solvent Self-Proliferating Process. *Regenerative Biomater.* 4, 233–242. doi:10.1093/rb/rbx014

Dias, D., Vale, A. C., Cunha, E. P. F., Paiva, M., Reis, R. L., Vaquette, C., et al. (2021). 3D -printed Cryomilled Poly(ε-caprolactone)/graphene Composite Scaffolds for Bone Tissue Regeneration. *J. Biomed. Mater. Res.* 109, 961–972. doi:10.1002/jbm.b.34761

Farokhi, M., Mottaghitalab, F., Samani, S., Shokrgozar, M. A., Kundu, S. C., Reis, R. L., et al. (2018). Silk Fibroin/hydroxyapatite Composites for Bone Tissue Engineering. *Biotechnol. Adv.* 36, 68–91. doi:10.1016/j.biotechadv.2017.10.001

Gholipourmalekabadi, M., Mozafari, M., Gholipourmalekabadi, M., Nazm Bojnordi, M., Hashemi-soteh, M. B., Salimi, M., et al. (2015). In Vitroandin Vivoevaluations of Three-Dimensional Hydroxyapatite/silk Fibroin Nanocomposite Scaffolds. *Biotechnol. Appl. Biochem.* 62, 441–450. doi:10.1002/bab.1285

Hassanajili, S., Karami-Pour, A., Oryan, A., and Talaei-Khozani, T. (2019). Preparation and Characterization of PLA/PCL/HA Composite Scaffolds Using Indirect 3D Printing for Bone Tissue Engineering. *Mater. Sci. Eng. C* 104, 109960. doi:10.1016/j.msec.2019.109960

Huang, T., Fan, C., Zhu, M., Zhu, Y., Zhang, W., and Li, L. (2019). 3D-printed scaffolds of biomineralized hydroxyapatite nanocomposite on silk fibroin for improving bone regeneration, *Applied Surface Science* 467-468, 345-353. doi:10.1016/j.apsusc.2018.10.166

Jin, J., Wang, J., Huang, J., Huang, F., Fu, J., Yang, X., et al. (2014). Transplantation of Human Placenta-Derived Mesenchymal Stem Cells in a Silk Fibroin/hydroxyapatite Scaffold Improves Bone Repair in Rabbits. *J. Biosci. Bioeng.* 118, 593–598. doi:10.1016/j.jbiosc.2014.05.001

Kambe, Y., Murakoshi, A., Urakawa, H., Kimura, Y., and Yamaoka, T. (2017). Vascular Induction and Cell Infiltration into Peptide-Modified Bioactive Silk Fibroin Hydrogels. *J. Mater. Chem. B* 5, 7557–7571. doi:10.1039/c7tb02109g

Larobina, D., Guarino, V., and Ambrosio, L. (2012). Modeling of Phase Separation Mechanism in Polycaprolactone/dioxane Binary Systems. *J. Appl. Biomater. Funct. Mater.* 10, 237–242. doi:10.5301/JABFM.2012.10363

Mazas, S., Benzakour, A., Castelain, J.-E., Damade, C., Ghailane, S., and Gille, O. (2019). Cervical Disc Herniation: Which Surgery?. *Int. Orthopaedics (Sicot)* 43, 761–766. doi:10.1007/s00264-018-4221-3

Ming, J., Jiang, Z., Wang, P., Bie, S., and Zuo, B. (2015). Silk Fibroin/sodium Alginate Fibrous Hydrogels Regulated Hydroxyapatite crystal Growth. *Mater. Sci. Eng. C* 51, 287–293. doi:10.1016/j.msec.2015.03.014

Park, J. H., and Roh, S. W. (2013). Anterior Cervical Interbody Fusion Using Polyetheretherketone Cage Filled with Autologous and Synthetic Bone Graft Substrates for Cervical Spondylosis: Comparative Analysis between PolyBone and Iliac Bone. *Neurol. Med. Chir.(Tokyo)* 53, 85–90. doi:10.2176/nmc.53.85

Pei, B., Wang, Z., Nie, J., and Hu, Q. (2019). Highly Mineralized Chitosan-Based Material with Large Size, Gradient mineral Distribution and Hierarchical Structure. *Carbohydr. Polym.* 208, 336–344. doi:10.1016/j.carbpol.2018.12.087

Pitjamit, S., Thunsiri, K., Nakkiew, W., Wongwichai, T., Pothacharoen, P., and Wattanutchariya, W. (2020). The Possibility of Interlocking Nail Fabrication from FFF 3D Printing PLA/PCL/HA Composites Coated by Local Silk Fibroin for Canine Bone Fracture Treatment. *Materials* 13, 1564. doi:10.3390/ma13071564

Ruan, S.-Q., Deng, J., Yan, L., and Huang, W.-l. (2018). Composite Scaffolds Loaded with Bone Mesenchymal Stem Cells Promote the Repair of Radial Bone Defects in Rabbit Model. *Biomed. Pharmacother.* 97, 600–606. doi:10.1016/j.biopha.2017.10.110

Su, X., Wang, T., and Guo, S. (2021). Applications of 3D Printed Bone Tissue Engineering Scaffolds in the Stem Cell Field. *Regenerative Ther.* 16, 63–72. doi:10.1016/j.reth.2021.01.007

Sun, K., Li, R., Jiang, W., Sun, Y., and Li, H. (2016). Comparison of Three-Dimensional Printing and Vacuum Freeze-Dried Techniques for Fabricating Composite Scaffolds. *Biochem. Biophysical Res. Commun.* 477, 1085–1091. doi:10.1016/j.bbrc.2016.07.050

Thunsiri, K., Pitjamit, S., Pothacharoen, P., Pruksakorn, D., Nakkiew, W., and Wattanutchariya, W. (2020). The 3D-Printed Bilayer's Bioactive-Biomaterials Scaffold for Full-Thickness Articular Cartilage Defects Treatment. *Materials* 13, 3417. doi:10.3390/ma13153417

Wei, L., Wu, S., Kuss, M., Jiang, X., Sun, R., Reid, P., et al. (2019). 3D Printing of Silk Fibroin-Based Hybrid Scaffold Treated with Platelet Rich Plasma for Bone Tissue Engineering. *Bioactive Mater.* 4, 256–260. doi:10.1016/j.bioactmat.2019.09.001

Conflict of Interest: The authors declare that the research was conducted in the absence of any commercial or financial relationships that could be construed as a potential conflict of interest.

Publisher's Note: All claims expressed in this article are solely those of the authors and do not necessarily represent those of their affiliated organizations, or those of the publisher, the editors and the reviewers. Any product that may be evaluated in this article, or claim that may be made by its manufacturer, is not guaranteed or endorsed by the publisher.